Journal of Biomedical Optics

SPIEDigitalLibrary.org/jbo

Femtosecond laser-induced fusion of nonadherent cells and two-cell porcine embryos

Kai Kuetemeyer
Andrea Lucas-Hahn
Bjoern Petersen
Heiner Niemann
Alexander Heisterkamp

SPIE

Femtosecond laser-induced fusion of nonadherent cells and two-cell porcine embryos

Kai Kuetemeyer,[a] Andrea Lucas-Hahn,[b] Bjoern Petersen,[b] Heiner Niemann,[b] and Alexander Heisterkamp[a]
[a]Laser Zentrum Hannover e.V., Hollerithallee 8, 30419 Hannover, Germany
[b]Friedrich-Loeffler-Institut, Institute of Farm Animal Genetics, Hoeltystrasse 10, 31535 Neustadt, Germany

Abstract. Cell fusion is a fundamental biological process that can be artificially induced by different methods. Although femtosecond (fs) lasers have been successfully employed for cell fusion over the past few years, the underlying mechanisms are still unknown. In our experimental study, we investigated the correlation between fs laser-induced cell fusion and membrane perforation, and the influence of laser parameters on the fusion efficiency of nonadherent HL-60 cells. We found that shorter exposure times resulted in higher fusion efficiencies with a maximum of 21% at 10 ms and 100 mJ/cm^2 (190 mW). Successful cell fusion was indicated by the formation of a long-lasting vapor bubble in the irradiated area with an average diameter much larger than in cell perforation experiments. With this knowledge, we demonstrated, for the first time, the fusion of very large parthenogenetic two-cell porcine embryos with high efficiencies of 55% at 20 ms and 360 mJ/cm^2 (670 mW). Long-term viability of fused embryos was proven by successful development up to the blastocyst stage in 70% of cases with no significant difference to controls. In contrast to previous studies, our results indicate that fs laser-induced cell fusion occurs when the membrane pore size exceeds a critical value, preventing immediate membrane resealing.
 [DOI: 10.1117/1.3609818]

Keywords: femtosecond laser; cell surgery; cell fusion; vapor bubble; membrane perforation; parthenogenetic embryo; somatic cell nuclear transfer.

Paper 11154R received Mar. 28, 2011; revised manuscript received Jun. 10, 2011; accepted for publication Jun. 20, 2011; published online Aug. 1, 2011.

1 Introduction

Cell-to-cell fusion (cell fusion) is a fundamental biological process in the development and physiology of multicellular organisms.[1] Since Okada discovered that cell fusion can be artificially induced by viruses *in vitro*,[2] it has become a powerful tool for analysis of gene expression, chromosomal mapping, antibody production, and cancer immunotherapy.[1] To date, cell fusion has been achieved by viruses, chemical substances,[3] and electrical[4] or laser pulses.[5] The mechanisms of cell fusion are still not fully understood. It is assumed that each method provides activation energy for the approach of both negatively charged outer membrane leaflets. Afterwards, the outer and inner leaflets fuse and a fusion pore is created, providing a channel for cytoplasmic streaming. This channel is continuously broadened until the fusion process is finished.[6]

Among the established methods, laser-induced cell fusion is the only noncontact method which can be combined with optical tweezers to selectively fuse two single cells in a culture dish.[7] This is generally done by targeted irradiation of the cell-cell junction between two aggregating cells.[5,7] Different cell types with volumes ranging from ~ 0.5 to 4 pl (somatic cells) to 15 to 30 pl (embryonic C.elegans and mouse cells) were successfully fused to this day.[5,7,8] However, fusion of very large cells, such as two-cell stage embryos of farm animals, has not yet been published.

The first systematic study by Sato et al. in 1992 used a nanosecond (ns) pulsed UV laser and achieved fusion efficiencies up to 50%.[9] Recently, mode-locked femtosecond (fs) Ti:Sapphire laser oscillators have also been successfully employed.[10] Over the past decade, they have proven to be an excellent tool for minimally invasive and extremely precise ablation of subcellular structures with cut sizes below 100 nm.[11–13] Compared to nanosecond laser pulses, much lower pulse energies on the order of some nanojoules are required, therefore minimizing the heat and mechanical energy transfer to surrounding regions. In this so-called low-density plasma regime, intracellular ablation is achieved by cumulative free electron and free radical-mediated chemical effects.[14] Although Gong et al. achieved very high fusion efficiencies around 80% with fs laser pulses, these results have to be taken with caution. In both mentioned studies using ns and fs laser pulses, polyethylene glycol (PEG) was added to the culture medium prior to irradiation to induce cell aggregation.[9,10] Previous work showed that this work step significantly increases the fusion efficiency.[7] Since PEG is also commonly used as a fusogen,[15] it is unclear if the high fusion efficiencies can be attributed to laser irradiation or PEG. To get a better understanding of the laser-cell interaction, it is thus advantageous to omit chemical substances in fs laser-induced cell fusion.

The mechanisms of fs laser-induced cell fusion are as yet almost unexplored. Gong et al. proposed that membrane perforation is not required for cell fusion,[10] as the fusion threshold irradiance was a factor 3 to 5 lower than generally used in cell perforation experiments.[16–18] Following their theoretical model, free electrons are captured by phospholipid molecules of both adjacent cell membranes.[10] As in other cell fusion

Address all correspondence to: Kai Kuetemeyer, Laser Zentrum Hannover e.V., Hollerithallee 8, Hannover, 30419 Germany; Tel: 00495112788361, Fax: 00495112788100; E-mail: k.kuetemeyer@lzh.de

1083-3668/2011/16(8)/088001/7/$25.00 © 2011 SPIE

methods, this process provides the activation energy for the approach of negatively charged outer membrane leaflets. However, Zimmermann concluded from their experiments with electrical pulses that cell perforation and fusion are very similar.[4] In both cases, the application of an electrical field results in dielectric breakdown of the membrane and a pore is created. In contrast to cell perforation experiments, it is assumed that the pore diameter has to exceed the critical value for permanent membrane instability to induce outer membrane leaflet fusion.[4] This is consistent with somatic cell nuclear transfer experiments, in which the electrical fields for cell fusion are higher than for membrane permeabilization.[19] Successful fs laser cell perforation is generally indicated by the formation of a long-lasting vapor bubble visible under conventional light microscopy.[17,18,20] These vapor bubbles are presumed to be attributed to accumulative heating and chemical disintegration of biomolecules.[14] Consequently, bubble formation is a suitable criterion for clarifying the need of membrane perforation for cell fusion.

Here, we investigated the influence of pulse energy and exposure time on the fusion efficiency of nonadherent HL-60 cells. The formation of long-lasting vapor bubbles was monitored using light microscopy to correlate cell fusion and membrane perforation. With this knowledge, we were able to fuse very large parthenogenetic two-cell porcine embryos with a cell volume of about 200 pl. Subsequent *in vitro* culture up to the blastocyst stage served as an indicator of long-term cell viability.

2 Materials and Methods

2.1 *Sample Preparation*

Nonadherent human promyelocytic leukemia cells (HL-60) were routinely grown in T25 vented-top culture flasks (Sarstedt) using RPMI 1640 medium (Roswell Park Memorial Institute) supplemented with 10% fetal calf serum, and the antibiotics penicillin and streptomycin at 37°C and 5% CO_2 humidified atmosphere. For fusion experiments, cells were seeded in 35-mm glass bottom dishes with a thickness of 170 μm (ibidi GmbH). The glass bottom dishes were placed into a microscope stage incubation system (Okolab), which was set to 37°C and 5% CO_2 humidified atmosphere.

The procedures and media used to obtain parthenogenetic two-cell porcine embryos have been described elsewhere.[21] About 24 h after parthenogenetic activation, embryos were transferred in groups of five to a drop of TL-Hepes 296 medium on a glass bottom dish, which was placed on a heating plate at 38°C.

2.2 *Optical Setup*

The optical setup is shown in Fig. 1. Femtosecond laser-induced cell fusion was investigated using a tunable Ti:sapphire laser oscillator emitting 140 fs pulses at 80 MHz repetition rate over a wavelength range of 680 to 1040 nm (Chameleon Ultra II, Coherent, Inc.). A wavelength of 720 nm was selected for the experiments as it provides an enhanced production of free electrons at high repetition rates.[22] The laser beam was magnified by a two-lens telescope to match the back aperture of the microscope objectives. After entering the tube of an inverted microscope (Axiovert 100, Carl Zeiss AG) via a dichroic mirror, the beam was focused into the sample by either a 40 × 0.8 NA

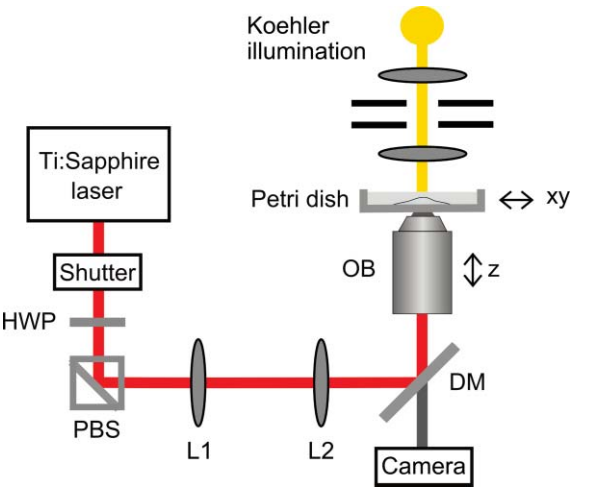

Fig. 1 Schematic setup for femtosecond laser-induced cell fusion. The tunable 80 MHz Ti:sapphire oscillator was set to a wavelength of 720 nm in all experiments. HWP: half-wave plate; PBS: polarizing beamsplitter cube; L1 and L2: 50 and 150 mm planoconvex lenses; DM: dichroic mirror; OB: high-NA objective.

water immersion objective (C-Achroplan NIR, Carl Zeiss AG) or a 20 × 0.5 NA air objective (EC Plan-Neofluar, Carl Zeiss AG). This resulted in a diffraction limited spot diameter of 1.1 and 1.8 μm, respectively. It is commonly understood that oil immersion objectives with high numerical apertures (NA ≥ 1) decrease the average laser power for cell surgery experiments. However, precise axial beam alignment and positioning on the plasma membrane, crucial for successful cell fusion, is less relevant at lower numerical apertures. In addition, fast objective switching is mandatory in many biomedical applications to stay on schedule, such as somatic cell nuclear transfer.[21]

A mechanical shutter (SH05, Thorlabs) was placed in the beam path to adjust the exposure time at the sample. Precise positioning of the sample in the *xy*-plane was achieved by a motorized stage system (H117 ProScan II, Prior Scientific). A Koehler illumination configuration yielded even illumination throughout the entire focal plane. Images were recorded with a CCD camera (CCD1300CB, VDS Vosskuehler GmbH) at 10 frames/s. A micropipette with an inner diameter of approximately 50 μm, connected to a syringe via a tube, was attached to the microscope to hold single embryos in position by applying a slight low pressure.

2.3 *Cell Fusion and Viability*

In fusion experiments with HL-60 cells, only cell pairs in close contact were selected for laser treatment, as the molecule exchange required for cell fusion is impeded at distances of more than 50 Å.[23] This preselection was not necessary for two-cell porcine embryos because of their inherent close contact. The cell-cell junction between HL-60 cells was moved into the laser focus by carefully adjusting the motorized stage system and the fine focus adjustment knob of the microscope. In the case of two-cell embryos, alternate low and high pressure was applied with the syringe until the cell-cell junction could be identified in the equatorial plane. Irradiation of the junction was done up

to 3 times at slightly different axial positions if no long-lasting vapor bubble was visible directly afterwards [see Fig. 2(b)].

Fusion efficiencies were evaluated 10 and 120 min after irradiation for HL-60 cells and two-cell porcine embryos, respectively. Short-term viability of fused cells was assessed after further incubation for 1 h by addition of 1 μg/ml Calcein AM (Invitrogen) and 5 μg/ml propidium iodide (Invitrogen). The acetomethoxy group of Calcein AM is removed in live cells by cellular esterases, making Calcein green fluorescent. Propidium iodide binds to double-stranded DNA, but it can only cross the plasma membrane of nonviable cells. Both fluorescence signals were detected using a multiphoton microscopy setup described in our recent paper.[22] Staining of nuclear DNA with 5 μg/ml Hoechst 33342 (Invitrogen) for 10 min was done to identify the nuclei of both cells in the fused complex.

To determine long-term viability, fused two-cell porcine embryos were cultivated in NCSU 23 medium supplemented with 0.4 mg/ml BSA for 6 more days at 38.5°C in 5% CO_2 in humidified air. Morphological criteria, including cell shape and blastocoele formation, were used to determine the successful development up to the blastocyst stage. To assess their ploidy, embryonic cells were arrested in metaphase with 0.5 μg/ml colcemid for 3 h. Thereafter, embryos were fixed for 24 h in a solution of methanol and acetic acid (3:1 ratio), stained with Giemsa and analyzed using phase contrast microscopy.

The statistical significance was tested using Student's t-test. Differences between experimental groups were considered significant at $P < 0.05$.

3 Results

3.1 *Fusion of HL-60 Cells*

The first set of experiments was made to identify laser parameter regimes suitable for femtosecond laser-induced fusion of HL-60 cells. To this end, the cell-cell junction was irradiated with different exposure times and pulse energies using a 0.8 NA water immersion objective. The laser fluence was thereby defined as the pulse energy divided by the focal area. At low fluences without immediate visual cellular response to laser irradiation, no signs of fusion or cell death were observed. Above a certain threshold depending on the exposure time ($\sim$ 80 to 120 mJ/cm^2 resp. 60 to 90 mW), a long-lasting vapor bubble with a lifetime up to 1 s was formed in the irradiated area [see Fig. 2(b)]. Only in this regime, three different outcomes occurred within a few minutes: 1. lack of cell fusion or other cellular response, 2. successful fusion, and 3. lack of cell fusion but significant cell morphology changes, granularity and death.

In the case of cell fusion, membrane fusion was clearly visible after 30 s [see Fig. 2(c)]. It took approximately 5 to 10 min until the fused cells rounded up. In some fused cell pairs, a small dark circular spot of about the same size as the focused laser beam appeared in the irradiated area directly after treatment, which faded within several minutes [see Figs. 2(d)–2(f)]. Independent of the laser parameters, fused cells were predominantly viable 1 h after fusion (>95%, 26 fused cells were analyzed in total), as indicated by bright Calcein AM fluorescence and lack of propidium iodide signal (data not shown).

The correlation between the size of the generated vapor bubble, its lifetime, and cell fusion probability was elucidated by

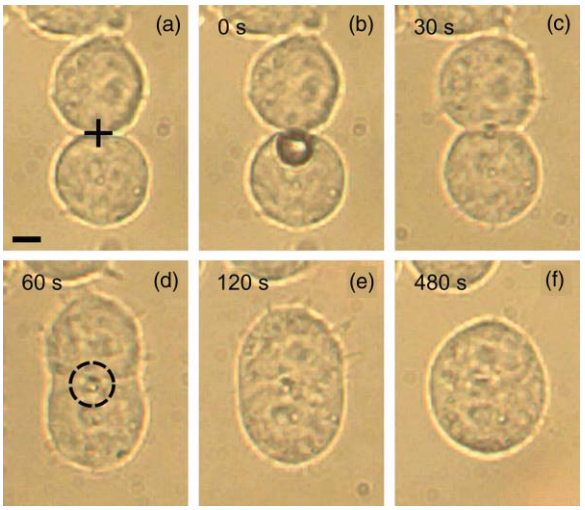

Fig. 2 Femtosecond laser-induced fusion of HL-60 cells using a 0.8 NA water immersion objective. (a) Above a certain threshold, irradiation of the cell-cell junction (indicated by black cross) resulted in a long-lasting vapor bubble (b). A small dark circular spot appeared in the treated area [indicated by dashed circle in (d)] and the HL-60 cell pair started to fuse about 30 s after irradiation (c). Cell fusion proceeded through intermediate stages (d) and (e) to reach completion in about 5 to 10 min (f). Scale bar: 5 μm.

analyzing 150 representative irradiated cell pairs above the bubble formation threshold. As the size of the bubble continuously decreased over time (data not shown), the maximum bubble diameter was defined by the corresponding value in the first CCD image after bubble formation. The maximum bubble diameter varied over a large range from 1.2 to 10 μm. However, its probability of occurrence continuously declined with increasing diameter [see dark bars in Fig. 3(a)]. High fusion rates were only obtained at diameters between 4 and 8 μm with ratios of 2 to 14 between fused and nonfused cells. For nonfused cells subjected to larger bubble formation (>5 μm), cell viability was often compromised, as indicated by morphology changes. Figure 3(b) shows a plot of the maximum bubble diameter (D) versus the corresponding bubble lifetime (t_L) with a time resolution of 100 ms. As expected, the bubble lifetime continuously increased with its diameter. The data was best fitted by a power function ($t_L = A \cdot D^k$) with a scaling exponent of $k = 1.7$.

The fusion efficiency of HL-60 cells was analyzed for exposure times of 10 and 60 ms at different laser fluences. The first value corresponds to the shortest possible exposure time with our setup, while the second value is often used in membrane perforation experiments.[18] Since the maximum fusion efficiencies were independent of the objective NA (data not shown), the 0.5 NA air objective with a larger field of view was used in this experiment. The fluence threshold for cell fusion was determined to $\sim$75 mJ/cm^2 (140 mW) for 10 ms and $\sim$55 mJ/cm^2 (105 mW) for 60 ms, and coincided with the respective bubble formation threshold. The fusion efficiency increased with the laser fluence for both exposure times until it peaked at 21% for 10 ms and 15% for 60 ms (see Fig. 4). The corresponding fluences were 45% and 70% above the threshold, respectively. A further increase of the laser fluence led to a steady decrease in the fusion probability for both exposure times. However, even at fluences more than 2 times the threshold, efficiencies were still

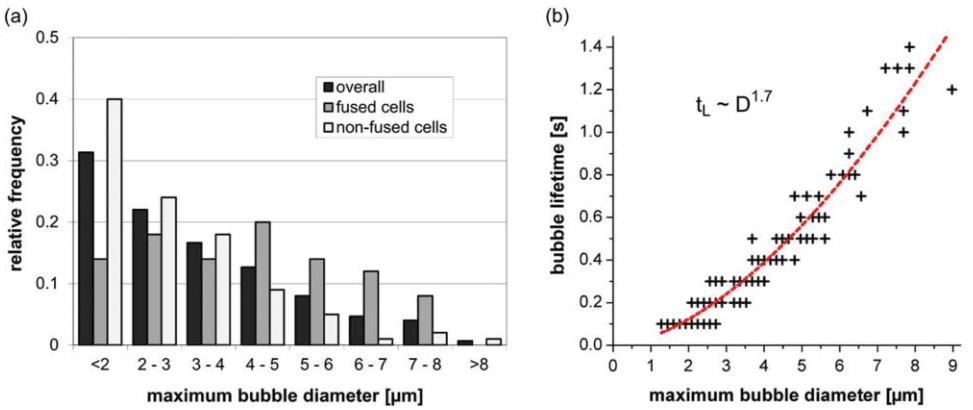

Fig. 3 (a) Histogram of the maximum vapor bubble diameter after laser irradiation of n=150 representative HL-60 cell pairs. Relative frequencies are shown for all irradiated cells (black bars), fused cells (gray bars), and nonfused cells (white bars). High fusion probabilities were only observed at diameters between 4 and 8 μm. (b) Vapor bubble lifetime (t_L) as a function of the maximum diameter (D) for $n = 150$ HL-60 cell pairs. The data was best fitted by a power function with a scaling exponent of $k = 1.7$. Cell fusion was induced by irradiation at 180 mJ/cm^2 (135 mW) laser fluence for 10 ms using a 0.8 NA water immersion objective.

in the range of 5% to 10%. By looking at the fluences scaled by the threshold, it is apparent that the corresponding fusion efficiency was always higher at the shorter exposure time [compare Figs. 4(a) and 4(b)].

3.2 *Fusion of Parthenogenetic Two-Cell Porcine Embryos*

Based on the results derived in Sec. 3.1, we investigated the fs laser-induced fusion of parthenogenetic two-cell porcine embryos, having a much larger diameter of ~150 μm. In all of these experiments, the 20 × 0.5 NA air objective with a larger field of view was employed. Because of the high cytoplasmic lipid content in porcine embryos, the light transmission is very low, especially in the near infrared wavelength range.[24] Therefore, the fluence threshold for fusion of two-cell porcine embryos was 3- to 4-fold higher (~ 180 to 280 mJ/cm^2 resp. 330 to 520 mW). Similar to HL-60 cells, the formation of a long-lasting vapor bubble in the irradiated area was necessary to induce cell fusion. On average, the bubble had a larger diameter up to 15 μm corresponding to a longer lifetime up to a few seconds. The intermediate stages of cell fusion were similar to those observed with HL-60 cells [compare Fig. 5(c)–5(e) and 2(d) and 2(e)], but took about a factor 20 longer to complete [compare Figs. 5(f) and 2(f)]. Not until approximately half an hour after irradiation, cytoplasmic streaming between both cells was clearly visible [see dashed circle in Fig. 5(b)].

To obtain fusion efficiencies as high as possible for a given exposure time, a laser fluence ~30% above the threshold was chosen at which a reproducible long-lasting vapor bubble was observed. The fusion efficiencies were analyzed for two exposure times of 20 and 100 ms at fluences of 230 and 360 mJ/cm^2 (430 and 670 mW), respectively [see Fig. 6(a)]. Although Sec. 3.1 clearly showed that even shorter exposure times are advantageous, we were thereby limited by the maximum pulse energy available from our Ti:sapphire laser. The percentage of

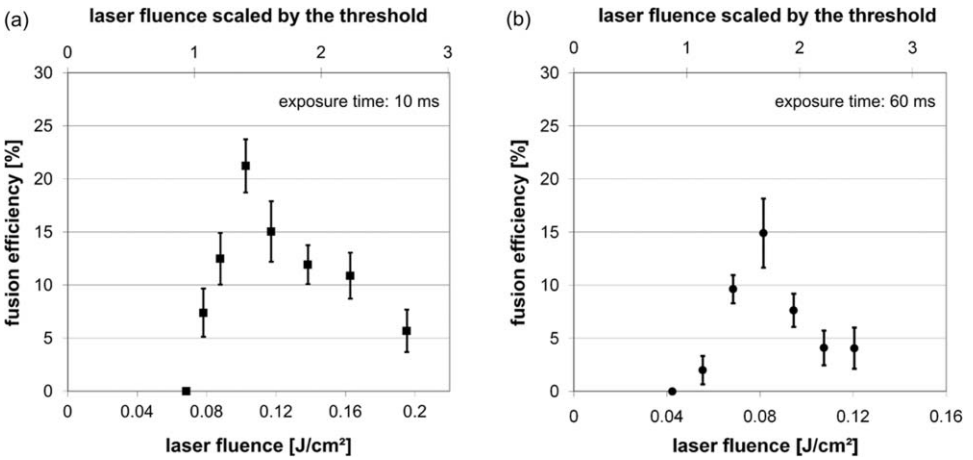

Fig. 4 Fusion efficiency data for the irradiation of n >2000 HL-60 cell pairs using a 0.5 NA air objective. Exposure times of (a) 10 ms and (b) 60 ms were applied, while laser fluences varied between 0.04 and 0.2 J/cm^2 (75 and 375 mW). The fusion threshold corresponded to the bubble formation threshold in each case. Maximum fusion efficiencies of 21% and 15% were obtained at 10 and 60 ms exposure time, respectively, at fluences about 50% above the fusion threshold. Fused cells were predominantly viable (>95%), independent of the laser parameters. Each data point represents the mean ± standard error of at least 5 experiments with more than 100 cell pairs in total.

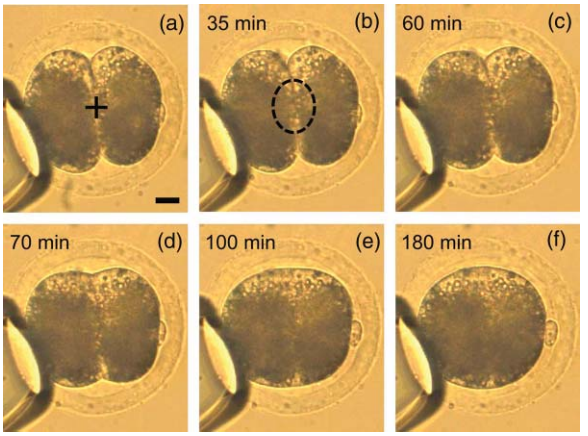

Fig. 5 Femtosecond laser-induced fusion of two-cell porcine embryos using a 0.5 NA air objective. (a) Irradiation of the cell-cell junction (indicated by black cross) initiated cell fusion. (b) Cytoplasmic streaming between both cells occurred about half an hour after laser treatment (indicated by dashed ellipse). (c)–(e) Cell fusion proceeded through the same intermediate stages as with HL-60 cells, but took about 20 times longer to complete (f). Scale bar: 20 μm.

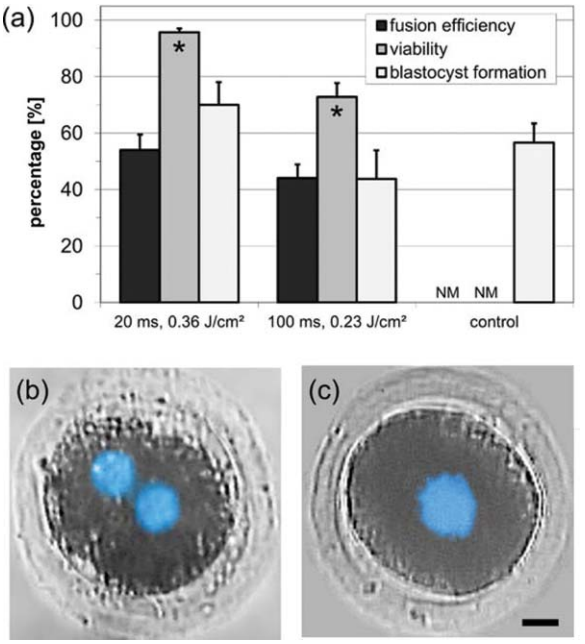

Fig. 6 (a) Evaluation of fusion efficiency, cell viability and blastocyst formation after laser irradiation of n >450 two-cell porcine embryos using a 0.5 NA air objective. Exposure times of 20 and 100 ms were used at laser fluences of 230 and 360 mJ/cm^2 (430 and 670 mW), respectively. At the shorter exposure time, a higher fusion efficiency and significantly higher viability were observed. No significant difference was found in the rates of blastocyst formation between fused and untreated control embryos. NM: not measured. Each bar represents the mean ± standard error of at least four experiments. The asterisks indicate that values are significantly different ($P < 0.05$). (b) and (c) Hoechst staining of fused embryos revealed that both nuclei (in blue) either (b) remained separated or (c) seemed to fuse within a few hours after laser treatment. Scale bar: 20 μm.

fused two-cell porcine embryos was slightly higher at 20 ms (54%) than at 100 ms exposure time (44%). At the same time, cell viability was significantly higher at the shorter exposure time (95% at 20 ms versus 73% at 100 ms, $P < 0.05$).

Following laser irradiation, fused two-cell porcine embryos were cultivated for 6 more days to determine the blastocyst rates. Similar to the fusion efficiency, the percentage of blastocyst formation was higher at 20 ms (70%) compared to 100 ms (43%) exposure time. No significant difference was observed between fused and control (no irradiation) embryos [$P > 0.13$, see Fig. 6(a)]. Hoechst staining of fused two-cell embryos exhibited two distinct fates of cell nuclei. They either remained separated in the cytoplasm or seemed to fuse in the middle of the embryo within a few hours [see Figs. 6(b) and 6(c)]. A ploidy analysis at the blastocyst stage revealed that only diploid cell nuclei were present in the first case, while several tetraploid cell nuclei were identified in the latter one (data not shown).

4 Discussion and Conclusion

The presented results provide new insights into the mechanisms of fs laser-induced cell fusion in the low-density plasma regime. To the best of our knowledge, this is the first study demonstrating a strong correlation between laser-induced cell fusion and membrane perforation. Furthermore, we achieved, for the first time, laser-induced fusion of parthenogenetic two-cell stage embryos of farm animals with cell volumes over 100 pl. As the indicators of successful cell fusion were the same for two distinct cell types with highly different cell volumes, the findings of this study can also be applied to other cell types.

Laser irradiation of the cell-cell junction between HL-60 cells and two-cell porcine embryos resulted in cell fusion above a certain fluence threshold (see Figs. 2 and 5). The fluence threshold depended both on the cell type and the exposure time (see Fig. 4). In all cases, it corresponded well to the threshold for vapor bubble formation with lifetimes up to one and a few seconds for HL-60 cells and two-cell porcine embryos, respectively. In fs laser cell perforation experiments, the formation of long-lasting vapor bubbles is an indicator for successful membrane permeabilization.[17,18,20] Therefore, our results suggest that membrane perforation is necessary for cell fusion. A systematic analysis of the maximum vapor bubble diameter revealed that high cell fusion probabilities were only obtained with diameters between 4 and 8 μm [see Fig. 3(a)]. These values are a factor of 2 to 4 higher than those for membrane perforation.[17] Similar observations have been made by Zimmermann in extensive studies using electrical pulses for membrane perforation and cell fusion.[4] Consequently, we presume that fs laser-induced cell fusion only occurs when the pore diameter exceeds a critical value preventing subsequent membrane resealing and favoring fusion of both outer membrane leaflets.

Immediately after laser irradiation and vapor bubble collapse, a small dark circular spot with about the same size as the laser focal spot appeared in the treated area, which faded within several minutes [see Fig. 2(d)]. This observation has also been made in membrane perforation experiments using cw laser and is attributed to a local transient increase in temperature.[25,26] For fs laser pulses, temperature calculations showed that pulse energies twice as high as the membrane perforation threshold are sufficient to reach the water boiling temperature in the focal volume after a few milliseconds with a series of pulses at 80 MHz repetition rate.[14] Since the fusion threshold is supposed to be above the therapeutic dosage for membrane perforation

(see previous paragraph), it is likely that thermal effects through heat accumulation are responsible for changing the optical properties of the irradiated area. This is supported by the strong correlation of the bubble lifetime and diameter [see Fig. 3(b)]. The experimental data was best fitted by a power function with a scaling exponent of $k = 1.7$. Previous studies have shown that the dynamics of cavitation bubbles is limited by liquid inertia, while thermal effects dominate the growth and collapse of vapor bubbles.[27] This results in a linear and quadratic dependence of the bubble lifetime on its diameter for cavitation and vapor bubbles, respectively.[28] Therefore, our results suggest that thermal effects play a significant role in the formation and dynamics of long-lasting vapor bubbles which is in good agreement with theoretical considerations by Vogel et al.[14]

The fusion efficiency depended on the cell type, laser fluence, and exposure time. While the percentage of fused HL-60 cells peaked at 21% [10 ms, 100 mJ/cm^2 (190 mW)], it was more than twice as high (54%) for two-cell porcine embryos [20 ms, 360 mJ/cm^2 (670 mW)], each at a fluence slightly above the fusion threshold [compare Figs. 4(a) and 6(a)]. At these laser parameters, fused cells of both cell types were predominantly viable (> 95%) 1 h after fusion. We assume that the main reasons for the difference in fusion efficiencies were the inherent close contact of both embryonic cells and their 20 times larger surface compared to somatic cells. Larger cells most likely have a higher resistance to vapor bubble formation, allowing for much larger bubble diameters.

For both cell types, the maximum fusion efficiency was higher at shorter exposure times of 10 and 20 ms compared to 60 and 100 ms, respectively. Further preliminary experiments over a large range of exposure times strongly indicate that the maximum fusion efficiency increases with decreasing exposure time. Based on our observations, we assume that this is attributed to the simultaneously decreasing variance of the bubble diameter (data not shown). By contrast, there seems to be an optimal exposure time for membrane perforation around 40 ms.[17,18,20] Further research is needed to elucidate this discrepancy.

In previous studies using laser pulses, higher fusion efficiencies up to 80% were achieved with somatic cells.[9,10] This can be explained by the addition of PEG to the culture medium which is a fusogen and improves cell aggregation.[7] Therefore, the average distance between both cells was higher in our study impeding the fusion of outer membrane leaflets. For parthenogenetic two-cell stage embryos, we achieved a fusion efficiency of 55% with porcine cells which is comparable to previous experiments with mouse cells (65%).[8]

Long-term viability of fused two-cell porcine embryos was demonstrated by successful development up to the blastocyst stage with no significant difference to controls [see Fig. 6(a)]. Therefore, laser irradiation had no apparent detrimental effects on the cytoplasm and nuclear DNA, both involved in cell division, which is in very good agreement with previous fusion experiments.[8] A ploidy analysis of embryos developed to the blastocyst stage revealed that tetraploid cells were present in some fused embryos at this stage (data not shown). This indicates that nuclear fusion may occur within a few hours after laser treatment [see Fig. 6(c)], which has also been observed with other cell fusion methods.[6]

In conclusion, we showed that fs laser-induced cell fusion is similar to cell perforation, independent of the cell type or volume. Successful cell fusion is indicated by the formation of a long-lasting vapor bubble in the irradiated area creating a pore in both adjacent cell membranes. In contrast to cell perforation, higher pulse energies and hence larger pores are required to induce cell fusion instead of membrane resealing. The high fusion efficiency (>50%) of two-cell porcine embryos combined with high long-term viability (70% blastocyst formation) is promising for biomedical applications, such as somatic cell nuclear transfer, in which a noncontact method is mandatory to selectively fuse two cells without the addition of chemical substances.

Acknowledgments

We thank Maren Ziegler, Erika Lemme, and Petra Hassel for their outstanding support in the lab. This work was supported by funding from the Deutsche Forschungsgemeinschaft (DFG, German Research Foundation) within the Cluster of Excellence "REBIRTH" (from Regenerative Biology to Reconstructive Therapy).

References

1. E. Chen and E. Olson, "Unveiling the mechanisms of cell-cell fusion," *Science* **308**, 369–373 (2005).
2. Y. Okada, "Analysis of giant polynuclear cell formation caused by HVJ virus from Ehrlich's ascites tumor cells: I. Microscopic observation of giant polynuclear cell formation," *Exp. Cell Res.* **26**, 98–107 (1962).
3. Q. Ahkong, F. Cramp, D. Fisher, J. Howell, and J. Lucy, "Studies on chemically induced cell fusion," *J. Cell Sci.* **10**, 769–787 (1972).
4. U. Zimmermann, "Electric field-mediated fusion and related electrical phenomena," *Biochim. Biophys. Acta* **694**, 227–277 (1982).
5. E. Schierenberg, "Altered cell-division rates after laser-induced cell fusion in nematode embryos," *Dev. Biol.* **101**, 240–245 (1984).
6. B. Ogle, M. Cascalho, and J. Platt, "Biological implications of cell fusion," *Nat. Rev. Mol. Cell Bio.* **6**, 567–575 (2005).
7. R. Steubing, S. Cheng, W. Wright, Y. Numajiri, and M. Berns, "Laser induced cell fusion in combination with optical tweezers: The laser cell fusion trap," *Cytometry* **12**, 505–510 (1991).
8. A. Karmenyan, A. Shakhbazyan, T. Sviridova-Chailakhyan, A. Krivokharchenko, A. Chiou, and L. Chailakhyan, "Use of picosecond infrared laser for micromanipulation of early mammalian embryos," *Mol. Reprod. Dev.* **76**, 975–983 (2009).
9. S. Sato, E. Higurashi, Y. Taguchi, and H. Inaba, "Achievement of laser fusion of biological cells using UV pulsed dye-laser beams," *Appl. Phys. B* **54**, 531–533 (1992).
10. J. Gong, X. Zhao, Q. Xing, F. Li, H. Li, Y. Li, L. Chai, Q. Wang, and A. Zheltikov, "Femtosecond laser-induced cell fusion," *Appl. Phys. Lett.* **92**, 093901 (2008).
11. K. Koenig, I. Riemann, and W. Fritzsche, "Nanodissection of human chromosomes with near-infrared femtosecond laser pulses," *Opt. Lett.* **26**, 819–821 (2001).
12. L. Sacconi, I.M. Tolic-Norrelykke, R. Antolini, and F.S. Pavone, "Combined intracellular three-dimensional imaging and selective nanosurgery by a nonlinear microscope," *J. Biomed. Opt.* **10**, 014002 (2005).
13. T. Shimada, W. Watanabe, S. Matsunaga, T. Higashi, H. Ishii, K. Fukui, K. Isobe, and K. Itoh, "Intracellular disruption of mitochondria in a living HeLa cell with a 76-MHz femtosecond laser oscillator," *Opt. Express* **13**, 9869–9880 (2005).
14. A. Vogel, J. Noack, G. Huettman, and G. Paltauf, "Mechanisms of femtosecond laser nanosurgery of cells and tissues," *Appl. Phys. B* **81**, 1015–1047 (2005).
15. R. Davidson and P. Gerald, "Improved techniques for induction of mammalian-cell hybridization by polyethylene-glycol," *Somatic. Cell Genet.* **2**, 165–176 (1976).

16. U. Tirlapur and K. Koenig, "Targeted transfection by femtosecond laser," *Nature (London)* **418**, 290–291 (2002).
17. D. Stevenson, B. Agate, X. Tsampoula, P. Fischer, C. Brown, W. Sibbett, A. Riches, F. Gunn-Moore, and K. Dholakia, "Femtosecond optical transfection of cells: viability and efficiency," *Opt. Express* **14**, 7125–7133 (2006).
18. J. Baumgart, W. Bintig, A. Ngezahayo, S. Willenbrock, H. Escobar, W. Ertmer, H. Lubatschowski, and A. Heisterkamp, "Quantified femtosecond laser based opto-perforation of living GFSHR-17 and MTH53a cells," *Opt. Express* **16**, 3021–3031 (2008).
19. B. Petersen, A. Lucas-Hahn, M. Oropeza, N. Hornen, E. Lemme, P. Hassel, A. Queisser, and H. Niemann, "Development and validation of a highly efficient protocol of porcine somatic cloning using preovulatory embryo transfer in peripubertal gilts," *Cloning Stem Cells* **10**, 355–362 (2008).
20. A. Uchugonova, K. Koenig, R. Bueckle, A. Isemann, and G. Tempea, "Targeted transfection of stem cells with sub-20 femtosecond laser pulses," *Opt. Express* **16**, 9357–9364 (2008).
21. M. Holker, B. Petersen, P. Hassel, W. Kues, E. Lemme, A. Lucas-Hahn, and H. Niemann, "Duration of in vitro maturation of recipient oocytes affects blastocyst development of cloned porcine embryos," *Cloning Stem Cells* **7**, 35–44 (2005).
22. K. Kuetemeyer, R. Rezgui, H. Lubatschowski, and A. Heisterkamp, "Influence of laser parameters and staining on femtosecond laser-based intracellular nanosurgery," *Biomed. Opt. Express* **1**, 587–597 (2010).
23. J. Wojcieszyn, R. Schlegel, K. Lumley-Sapanski, and K. Jacobson, "Studies on the mechanism of polyethylene glycol-mediated cell fusion using fluorescent membrane and cytoplasmic probes," *J. Cell Biol.* **96**, 151–159 (1983).
24. R. Zeggari, B. Wacogne, C. Pieralli, C. Roux, and T. Gharbi, "A full micro-fluidic system for single oocyte manipulation including an optical sensor for cell maturity estimation and fertilisation indication," *Sens. Actuators B* **125**, 664–671 (2007).
25. G. Palumbo, M. Caruso, E. Crescenzi, M. Tecce, G. Roberti, and A. Colasanti, "Targeted gene transfer in eucaryotic cells by dye-assisted laser optoporation," *J. Photochem. Photobiol., B* **36**, 41–46 (1996).
26. H. Schneckenburger, A. Hendinger, R. Sailer, W. Strauss, and M. Schmitt, "Laser-assisted optoporation of single cells," *J. Biomed. Opt.* **7**, 410–416 (2002).
27. M. Plesset and A. Prosperetti, "Bubble dynamics and cavitation," *Ann. Rev. Fluid. Mech.* **9**, 145–185 (1977).
28. L. Florschuetz and B. Chao, "On mechanics of vapor bubble collapse," *J. Heat Transfer* **87**, 209–220 (1965).